Journal of Alloys and Compounds 408–412 (2006) 593–597

Journal of ALLOYS AND COMPOUNDS

www.elsevier.com/locate/jallcom

Electron microscopic study on $SrGdMnO_4$

Hiromi Nakano [a,*], Nobuo Ishizawa [b], Naoki Kamegashira [c], Zulhadjri [c], Toetsu Shishido [d]

[a] Ryukoku University, Seta, Otsu 520-2194, Japan
[b] Nagoya Institute of Technology, 10-6-29 Asahigaoka, Tajimi 507-0071, Japan
[c] Toyohashi University of Technology, Tempaku-cho, Toyohashi 441-8580, Japan
[d] IMR in Tohoku University, Sendai 980-8577, Japan

Received 30 July 2004; received in revised form 27 September 2004; accepted 15 December 2004

Abstract

Single crystals of $SrGdMnO_4$ have been synthesized by the floating zone method. The structure was characterized as the K_2NiF_4-type, using X-ray diffraction (XRD) and a transmission electron microscope (TEM). Presence of weak reflections breaking the archetypal tetragonal symmetry was observed from the selected area diffraction (SAD). The compound was found to have an orthorhombic unit cell of $a \cong b = 0.532(4)$ nm, $c = 1.271(6)$ nm, by taking the a and b axes along the diagonal directions on the basal plane of the tetragonal archetype. Structural change occurred around 1018 K. The weak reflections disappeared in the SAD pattern, suggesting that crystal is of the archetype above 1018 K.

Keywords: Crystal growth; Transmission electron microscopy; X-ray diffraction; Crystal structure and symmetry

1. Introduction

Compounds of (La, Sr)$_2$MO$_4$ (M = Mn, Cu, Ni, Cr or Fe) with the K_2NiF_4-type structure have been the focus of research attention due to their electric and magnetic behaviours. Crystals of $La_{2-x}Sr_xMnO_4$ with $0.7 \le x \le 1.2$ were reported to take a tetragonal structure with the space group of *I4/mmm* [1]. Omata et al. prepared ceramics of $La_{2-x}Sr_xMnO_4$ with a wider range of $1.0 \le x \le 2.0$ and reported the lattice parameters and electrical conductivities [2]. Benabad et al. reported that the compounds of $SrLnMnO_4$ (Ln = La, Nd, Sm and Gd) take the K_2NiF_4-type structure with c/a ratios ranging from 3.445 to 3.428 [3].

In recent years, modifications having lower symmetries than that of the archetypal *I*4/*mmm* have been reported for the K_2NiF_4-type structure. For example, $La_{1.54}Sr_{0.46}NiO_4$ and $La_{1.91}Sr_{0.09}CuO_{4.12}$ take the monoclinic [4] and orthorhombic [5] structures, respectively. The structure relationship and phase transitions among these modifications and the archetype have been investigated and discussed in terms of the octahedral tilting system [6–9].

Recently, we succeeded in synthesizing a new compound $SrGdMnO_4$ by the floating zone method [10]. Structural characterization of the compound was thus performed using X-ray diffraction (XRD), and transmission electron microscope (TEM) with energy-dispersive spectroscopy (EDS).

2. Experimental procedure

Starting materials of high-purity (99.9%) $SrCO_3$, Gd_2O_3 and Mn_2O_3 went through the heat treatment for purification before weighing. These materials were mixed in an agate mortar in a stoichiometric composition of Sr:Gd:Mn being equal to 1:1:1. The mixture was compressed in a rubber tube into a rod shape under hydrostatic pressures. The rod was heated at 1273 K for 9 h in Ar gas atmosphere, and then at

---

* Corresponding author. Tel.: +81 77 543 7774.
E-mail address: hiromi@rin.ryukoku.ac.jp (H. Nakano).

0925-8388/$ – see front matter © 2005 Elsevier B.V. All rights reserved.
doi:10.1016/j.jallcom.2004.12.181

1673 K for 48 h. The obtained product was confirmed to be a single phase of polycrystalline $SrGdMnO_4$ by XRD. The rod was placed in a floating zone (FZ) furnace equipped with the bi-ellipsoidal halogen lamp. Crystals were grown from the melt at the growth rate of 20 mm/h. Details of the growth experiment will be published elsewhere [10]. Crystals used for the present study are as-grown crystals except for the quench experiment described in Section 3.2. The quenched sample used in 3.2 was annealed in a 1% H_2–Ar atmosphere at 1273 K for 5 days, followed by rapid quenching to room temperature.

The crystal was crushed into powder for powder XRD experiment. The crushed specimen was scooped with carbon-coated copper microgrids for the TEM observation. The TEM (JEOL-3000F) can provide electron probes with a full width at half maximum of around 0.5 nm as well as a sufficiently high current for the point- and mapping-analyses by EDS.

The in situ observation was performed using a thermal stage in TEM (JEM-2000EX, EM-SHTH specimen holder, Japan). The temperature of the stage was controlled manually from room temperature to 1018 K with a heating rate of approximately 973 K/h. The temperature was kept at 973 K for 30 min, and again increased to 1018 K. The observation was done at 673, 973 and 1018 K.

3. Results and discussion

3.1. Symmetry

The stability of the A_2BX_4-structure is often discussed in terms of the tolerance factor t [11]. The t-values of various K_2NiF_4-type compounds fall in the range of $0.8 < t < 1.0$ [9]. When t approaches the lower limit, the structure is subject to distortion and the symmetry changes from tetragonal to orthorhombic or monoclinic [9]. The t-value of 0.881 for $SrGdMnO_4$ is slightly smaller than 0.901 for $LaSrMnO_4$ with archetypal K_2NiF_4 structure [9].

Powder X-ray diffraction pattern of $SrGdMnO_4$ showed that the peaks could be indexed based on a tetragonal unit cell with lattice parameters $a = 0.532(4)$ nm and $c = 1.271(6)$ nm. Although the electron microscopy experiments revealed a faint but clear sign of symmetry changes from tetragonal to orthorhombic as described later, the difference between the a and b lengths was too small to be detected by the use of conventional powder XRD.

Geometrical relationship of the present crystal to the underlying archetypal structure with unit cell vectors $\boldsymbol{a}_t$, $\boldsymbol{b}_t$ and $\boldsymbol{c}_t$ can be given as $\boldsymbol{a}_t = (\boldsymbol{a} - \boldsymbol{b})/2$, $\boldsymbol{b}_t = (\boldsymbol{a} + \boldsymbol{b})/2$ and $\boldsymbol{c}_t = \boldsymbol{c}$. The space group of the archetype can be converted from $I4/mmm$ to $F4/mmm$ when the unit cell vectors are taken along the same directions as the present crystal.

Typical SAD patterns of the compound are shown in Fig. 1a–c, which were taken from [0 0 1], $[\bar{1}\,1\,0]$ and $[2\,1\,\bar{1}]$ zone axes, respectively. The reflections with strong intensities satisfy a condition, $h\,k\,l$ all even or all odd, and are those allowed for the $F4/mmm$ symmetry. On the other hand, the SAD patterns in Figs. 1a and 2c indicate a presence of extra reflections with weak intensities which do not conform to the archetypal symmetry. Presence of 1 2 0 and 2 1 0 reflections in Fig. 1a disagrees with the $P4_2/ncm$ symmetry reported for La_2CuO_4 [7], which excludes the $h\,k\,0$ reflections with $h + k$ odd. Possibility of the double diffraction effect was examined but ended with a conclusion that this was not the case for the 1 2 0 and 2 1 0 reflections. Detailed, though limited, search to find systematic extinction rules was performed from the SAD patterns. The 1 1 0, 1 0 1 and 0 1 1 reflections were not observed. The apparent presence of $0\,k\,0$ and $h\,0\,0$ reflections with h and k taking odd numbers in the [0 0 1] zone axis SAD pattern were explained by the double diffraction effect because no such reflections were observed in the $[0\,\bar{1}\,0]$ and $[\bar{2}\,0\,1]$ zone axis SAD patterns. The series of $0\,0\,l$ reflections with l odd were systematically absent as shown in Fig. 1b. The $h\,0\,l$, $0\,k\,l$ reflections with l odd were also systematically absent.

Orthorhombicity of the crystal was examined by measuring the distances of $(2\,0\,0)^*$ and $(0\,2\,0)^*$ in Fig. 1a using vernier calipers. The measurement was referenced to the polycrystalline rings of the Au film. The ratio of the $(0\,2\,0)^*/(2\,0\,0)^*$ spacing was thus determined to be

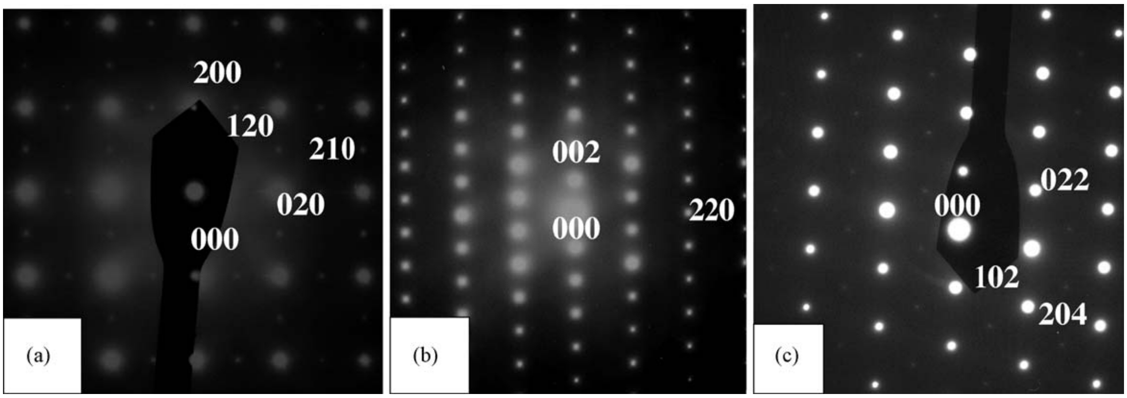

Fig. 1. Typical SAD patterns of $SrGdMnO_4$ taken from (a) the [0 0 1] zone axis, (b) $[\bar{1}\,1\,0]$ and (c) $[2\,1\,\bar{1}]$.

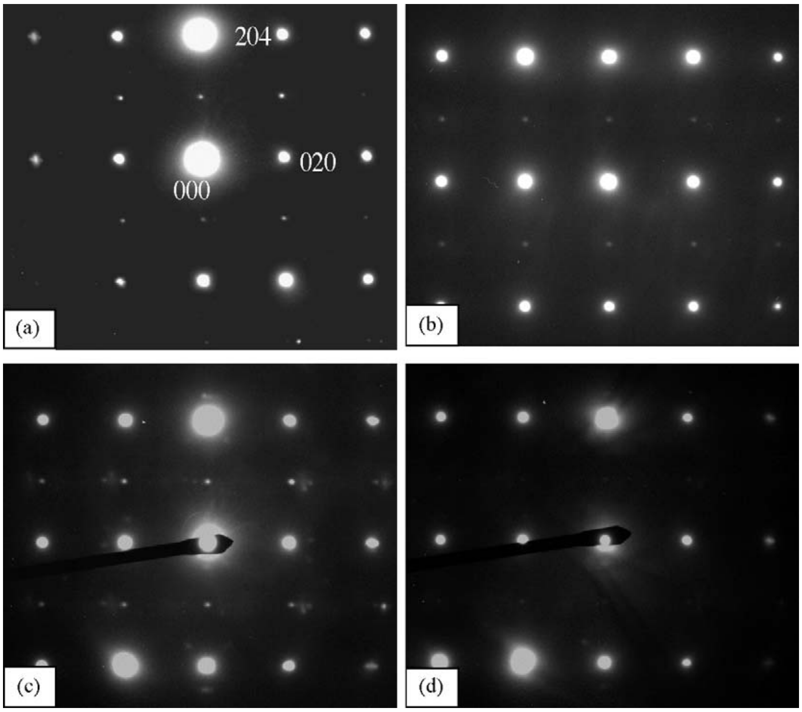

Fig. 2. Changes in SAD patterns of $SrGdMnO_4$ heated in TEM device at: (a) room temperature, (b) 673 K, (c) 973 K and (d) 1018 K.

0.994, suggesting a possible orthorhombic distortion for $SrGdMnO_4$. If the crystal is orthorhombic, these extinction rules uniquely lead to *Pccm* as a possible space group for $SrGdMnO_4$ at room temperature.

Aleksandrov [8] carried out a crystallographic analysis on the possible structural variants in the A_2BX_4 family arising from the tilting of BX_6 octahedra. In addition to the octahedral tilting, the Jahn–Teller (J–T) distortion accompanies in the case of $Mn^{3+}O_6$. This effect manifests itself in the changes of unit cell size and the c/a ratio in $Sr_{1+x}La_{1-x}MnO_4$ ($0 < x < 1$) [3]. In $SrGdMnO_4$, the cation valence can be assumed as Sr^{2+}, Gd^{3+} and Mn^{3+}. If a d^4 high spin state is assumed for the electron configuration of Mn^{3+}, the crystal field can be stabilized by the tetragonal elongation of the coordinating O_6 octahedron along the c-axis. This sort of J–T distortion, however, may contribute little to the symmetry changes from tetragonal to orthorhombic. Therefore, the appearance of weak reflections on the a^*–b^* plane should be related to the tilting of MnO_6 octahedra, and accordingly to the orthorhombic *Pccm* distortion.

In the case of $BaLnMnO_4$ (Ln = Pr or Nd), a similar unit cell of 0.5 nm × 0.5 nm × 1.2 nm to $SrGdMnO_4$ was reported [12,13]. However, the [0 0 1] zone axis SAD pattern of $BaPrMnO_4$ [13] is different from the present crystal in that the 1 1 0 reflection is absent in $SrGdMnO_4$.

In the copper-bearing K_2NiF_4-type structures, i.e., La_2MO_4 (M = Cu, Ni) [14–17] and $La_{2-x}Ba_xCuO_4$ [18,19], various space groups have been reported so far. We have noticed that our electron diffraction data are essentially the same as those of $La_{1.9}Ba_{0.1}CuO_4$ [19] with the orthorhombic *Pccm* structure. A detailed single crystal X-ray diffraction analysis is being undertaken.

3.2. Structural transition at high temperatures

The structural phase transition in $SrGdMnO_4$ was investigated with increasing temperature by TEM. Fig. 2 shows SAD patterns taken from $[\bar{2}\,0\,1]$ at room temperature in (a), 673 K in (b), 973 K in (c) and 1018 K in (d) using the as-grown crystal. The weak reflections disappeared at 1018 K. These findings show that a structural transition occurs from orthorhombic to tetragonal around 1018 K and the crystal takes the archetypal structure above that temperature.

Similar disappearance was confirmed in a quenched specimen at room temperature. Fig. 3 shows SAD patterns of the quenched specimen taken from the [0 0 1] zone axis in (a) and $[\bar{1}\,0\,0]$ in (b). No weak reflections forbidden for *F*4/*mmm* were observed between the parent reflections underlying the archetype structure.

3.3. Microstructure

The microstructure of $SrGdMnO_4$ as-grown crystals was analyzed by SEM–EDS and TEM–EDS. This was done because the Sr component is apt to vaporize in Sr-bearing compounds in the course of melt-growth owing to its high vapor pressure at elevated temperatures.

Fig. 4 is a TEM image of a crushed specimen of this compound. The two regions enclosed by circles in the figure were found to have different chemical compositions. As

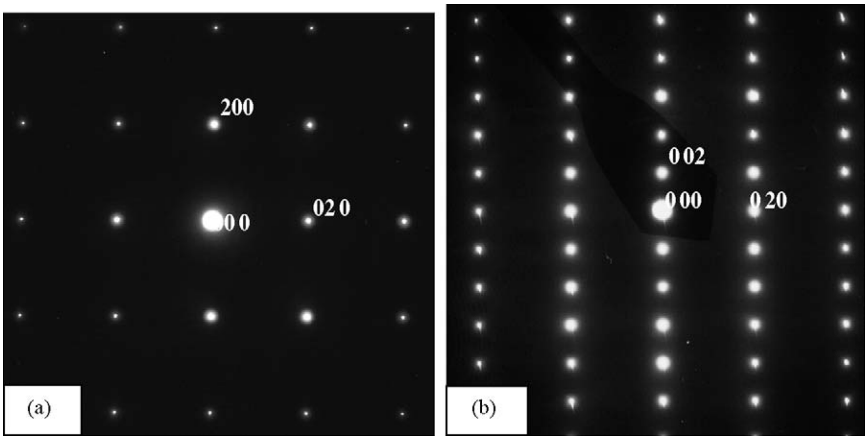

Fig. 3. SAD patterns of quenched $SrGdMnO_4$ taken from (a) the [1 0 0] zone axis and (b) [$\bar{1}$ 0 0].

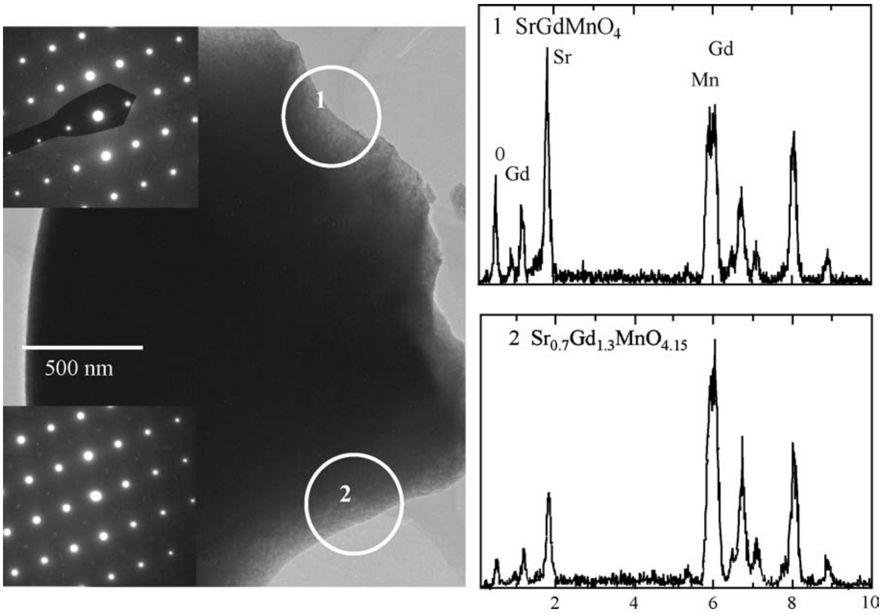

Fig. 4. TEM image of $SrGdMnO_4$ involving two regions with different chemical compositions enclosed by the circles. Insets are corresponding SAD patterns.

shown in the EDS spectra in Fig. 4, the region 1 was estimated to be a stoichiometric $SrGdMnO_4$ 1:1 composition while the region 2 is Sr-deficient with an estimated composition of $Sr_{0.7}Gd_{1.3}MnO_{4.15}$. In spite of difference in Sr content in these two regions, the SAD patterns are similar as shown in the insets of Fig. 4, suggesting an isomorphous structure for these regions. It is also notable that no clear boundary between them was detectable from this study.

4. Conclusions

Crystals of $SrGdMnO_4$ were prepared by the floating zone method. The structure was investigated by X-ray diffraction and transmission electron microscopy. Presence of extra reflections with weak intensities was detected between the present strong reflections underling the archetypal K_2NiF_4 structure with tetragonal *I*4/*mmm* symmetry. The extinction rules of $SrGdMnO_4$ at room temperature resemble those of $La_{1.9}Ba_{0.1}CuO_4$ with the orthorhombic *Pccm* structure.

A structural phase transition was observed around 1018 K for $SrGdMnO_4$ on the thermal stage in TEM device. The SAD pattern of the specimen above 1018 K showed the disappearance of the extra reflections with weak intensities, indicating that the high temperature phase is of *I*4/*mmm* archetype. A similar absence of the extra reflections with weak intensities was also confirmed in the quenched specimen at room temperature.

Most part of the crystal was identified to have a stoichiometric composition of $SrGdMnO_4$, nevertheless a Sr-deficient region was found occasionally. The chemical composition of the region was determined to be $Sr_{0.7}Gd_{1.3}MnO_{4.15}$ whose symmetry was supposed to be the same as that of $SrGdMnO_4$.

References

[1] I. Shimono, H. Konishi, J. Ceram. Soc. Jpn. 100 (1992) 1343 (in Japanese).
[2] T. Omata, S. Hoshino, H. Ikawa, T. Sasamoto, J. Ceram. Soc. Jpn. 103 (1995) 1297 (in Japanese).
[3] A. Benabad, A. Daoudi, R. Salmon, G. Leflen, J. Solid State Chem. 22 (1977) 121 (in French).
[4] P.J. Heaney, A. Mehta, G. Sarosi, V.E. Lamberti, A. Navrotsky, Phys. Rev. B 57 (17) (1998) 10370.
[5] C. Rial, E. Moran, M.A. Alario-Franco, U. Amador, N.H. Anderson, Physica C 254 (1995) 233.
[6] D.M. Hatch, H.T. Stokes, Phys. Rev. B 35 (16) (1987) 8509.
[7] K.S. Aleksandrov, I.N. Flerov, S.V. Melenikova, A.I. Kuglik, S.V. Misyul, O.A. Ageev, Ferroelectrics 104 (1990) 285.
[8] K.S. Aleksandrov, Sov. Phys. Crystallogr. 32 (4) (1987) 551.
[9] P. Ganguly, C.N.R. Rao, J. Solid State Chem. 53 (1984) 193.
[10] N. Kamegashira, in preparation.
[11] G.H. Jonker, J.H. van Santen, Physica 16 (1950) 337.
[12] N. Kamegashira, S. Ueno, H. Nakano, K. Enami, Mater. Res. Bull. 29 (2) (1994) 185.
[13] S. Ueno, K. Iwasaki, N. Kamegashira, H. Nakano, K. Enami, Mater. Chem. Phys. 42 (1995) 201.
[14] P. Odier, M. Le Blanc, J. Choisnet, Mater. Res. Bull. 21 (1986) 787.
[15] P. Zolliker, D.E. Cox, J.B. Parise, E.M. Mac Carron, Phys. Rev. B Condens. Matter 42 (10) (1990) 6332.
[16] T. Kajitani, T. Onozuka, Y. Yamaguchi, M. Hirabayashi, S. Yashuhiko, Jpn. J. Appl. Phys. Part 2 26 (1987) 1877.
[17] K. Yamada, E. Kudo, Y. Endoh, K. Tsuda, M. Tanaka, H. Asano, F. Izumi, M. Oda, Y. Hidaka, M. Suzuki, Jpn. J. Appl. Phys. Part 1 27 (1988) 1132.
[18] S. Katano, J.A. Ferrnandez-Baca, S. Funahashi, N. Mori, Y. Ueda, K. Koga, Physica C 214 (1993) 64.
[19] Y. Hirotsu, S. Nagakura, Y. Murata, T. Nishihara, M. Takata, T. Yamashita, Jpn. J. Appl. Phys. Part 2 26 (1987) 380.